A Redox Responsive, Fluorescent Supramolecular Metallohydrogel Consists of Nanofibers with Single-Molecule Width

Ye Zhang[1], **Bei Zhang**[2], **Yi Kuang**[1], **Yuan Gao**[1], **Junfeng Shi**[1], **Xixiang Zhang**[2], and **Bing Xu**[1,*]

[1]Department of Chemistry, Brandeis University, 415 South St., Waltham, MA 02454, USA

[2]Advanced Nano-fabrication, Imaging & Characterization Core Lab, King Abdullah University of Science and Technology, Thuwal 23955-6900, Saudi Arabia

Abstract

The integration of a tripeptide derivative, which is a versatile self-assembly motif, with a ruthenium(II)tris(bipyridine) complex affords the first supramolecular metallo-hydrogelator that not only self-assembles in water to form a hydrogel, but also exhibits gel-sol transition upon oxidation of the metal center. Surprisingly, the incorporation of the metal complex in the hydrogelator results in the nanofibers, formed by the self-assembly of the hydrogelator in water, to have the width of a single molecule of the hydrogelator. These results illustrate that metal complexes, besides being able to impart rich optical, electronic, redox or magnetic properties to supramolecular hydrogels, offer a unique geometrical control to pre-arrange the self-assembly motif prior to self-assembling. The use of metal complexes to modulate the dimensionality of intermolecular interactions may also help elucidate the interactions of the molecular nanofibers with other molecules, thus facilitating the development of supramolecular hydrogel materials for a wide range of applications.

This communication reports the incorporation of a metal complex in a hydrogelator for the development a redox responsive, fluorescent supramolecular hydrogel consisting of nanofibers resulted from one-dimensional (1D) intermolecular interactions. As the result of molecular self-assembly[1] driven by multiple non-covalent interactions in water, supramolecular hydrogels[2,3] formed by small molecules[4] have received considerable attentions recently because they promise soft materials with various important applications in biomedicines, such as drug delivery,[5,6] cell culture,[7] and sensors.[8] These supramolecular hydrogelators are usually organic molecules,[2] and a large portion of them are peptides or peptide derivatives.[9] Unlike the case of hydrogels, it is relatively common to utilize metal complexes as organogelators in the development of organogels[10] due to their rich optical, electronic, redox, or magnetic properties usually associated with metal centers and the stability of metal complexes in common organic solvents. For example, metal complex-based organogelators have exhibited a wide range of interesting properties, such as anion binding,[11] fluorescence,[12] color switch,[13] catalysis,[14] and responses to ultrasound,[15] redox perturbation,[16] or temperature.[17] Encouraged by these successful developments of organogelators made of metal complexes, we choose to develop hydrogelators containing

metal complexes and refer this type of hydrogelator as metallo-hydrogelators, which is a type of rarely explored building blocks of supramolecular hydrogels[18] despite the aforementioned properties of metal complexes.

In this work, we choose the ruthenium(II)tris(bipyridine) $[Ru(bipy)_3]^{2+}$ derivative as the metal complex for making metallo-hydrogelators because of its octahedral geometry and rich functions (e.g., as photocatalysts, as building blocks for conducting polymers, as DNA probes, or as fluorophores for electrochemoluminescence).[19] Although $[Ru(bipy)_3]^{2+}$ has served as the components for organogelators,[20] it has yet to be integrated with peptides to form supramolecular hydrogels. Thus, we design and synthesize a ruthenium(II)tris(bipyridine) complex (**3**) that bears a molecular motif (**1**) known to promote self-assembly in water.[6] While the ligand (**2**) itself fails to form a supramolecular hydrogel, the complex (**3**) acts as a metallo-hydrogelator that forms nanofibers at an exceptionally low critical concentration (0.00625% (w/v)) and supramolecular hydrogels over a wide pH range (pH 1 to 10). Being excited at 470 nm, the hydrogels of **3** exhibit an intense fluorescence with a maximum at 630 nm. Upon oxidation of the ruthenium from Ru(II) to Ru(III), the nanofibers of **3** break down to turn the hydrogel into a solution, accompanying by significant decrease of the circular dichroism (CD) signal. Most intriguingly, high-resolution transmission electron micrograph (HRTEM) indicates that the self-assembly of **3** results in the nanofibers of **3** to have the width of a single molecule of **3**. This result suggests that the geometry associated with $[Ru(bipy)_3]^{2+}$ favors one-dimensional intermolecular interactions of **3**, thus limiting the width of the supramolecular nanofibers of **3**. This subtle yet previously unknown observation related to metal complexes may lead a facile approach for designing new type of supramolecular nanofibers based on the geometries (e.g., octahedral, square planar, etc.) of metal complexes, which usually are unattainable by simple organic molecules alone. In addition, being more biocompatible than common polypyridyl ruthenium complex,[21] **3** also promises applications in molecular imaging.[22]

Scheme 1 shows the chemical structures of the molecular motif (**1**) known to self-assemble in water,[6] the ligand (**2**) consisting of a bipyridine and **1**, and the metallo-hydrogelator (**3**). After being obtained through solid-phase synthesis according to the reported procedure,[6] **1** reacts with 4,4′-dicarboxyl-2,2′-bipyridine[23] to afford the ligand (**2**) in 56% yield (Scheme S1). However, **2** is unable to form a supramolecular hydrogel upon changing pH or temperature. The aggregation of **2** only results in some precipitates, suggesting strong intermolecular interactions among the molecules of **2**. The organic functional groups (i.e., carboxylates or amides) appear to prevent **2** to react directly with a known polypyridyl ruthenium complex, [Ru(bipy)2]Cl2,[24] for making **3**. Thus, we use Ru(II)(bipy)2(4,4′-dicarboxyl-2,2′-bipyridine)dicholoride to react with **1** to form **3** in a moderate yield (Scheme S2). **3** is able to form hydrogels over a wide range of pH at various concentrations. For example, at pH = 1, it forms a soft gel at concentration of 0.1% (w/v) and a firm gel at concentration of 0.4% (w/v) (Fig. S1). At pH = 7, it forms a soft gel at concentration of 0.2% (w/v) and a firm gel at concentration of 0.8% (w/v) (Fig. 1A, Fig. S2). These results agree with that the protonation of the carboxyl groups on **3** at low pH decreases the solubility of **3**, and thus favors the formation of hydrogels. Being consistent with the well-known photochemical properties of $[Ru(bipy)_3]^{2+}$, the hydrogel of **3** exhibits strong fluorescence upon the irradiation of UV light (Fig. 1A). According to its absorbance (Fig. S8) and fluorescent spectrum (Fig. 1B), the hydrogel of **3**, being excited at 470 nm, fluoresces with the emission maximum at 630 nm. Being placed between a pair of crossed polarizers, the hydrogel of **3** also shows birefringence (Fig. 1A). Because the hydrogel of **1** lacks this interesting property, the anisotropy of the hydrogel of **3** likely relates to the incorporation of $[Ru(bipy)_3]^{2+}$ in **3**.

Hydrogelator **3** preserves the redox property of a polypyridyl ruthenium complex. Using $Ce(SO_4)_2$ to oxidize the hydrogel of **3**, we obtain a yellow emulsion during the process, and it eventually turns to transparent solution (Fig. 2A) that is not fluorescent (Fig. S5). Figure 2A shows the HRTEM images of the samples at different stages of the oxidation carried out at acidic condition (pH 1). At the reduced state (Ru(II)), the hydrogel of **3** consists of long and relatively flexible nanofibers that have the diameter of about 3 nm and entangle with each other to form a network. When the hydrogel turns to the yellow emulsion during the oxidation, TEM reveals that the network of the nanofibers breaks apart, and only scattered short nanofibers (about 3 nm in diameter and less than 30 nm in length) exist. When the emulsion turns to the transparent solution at the final stage of oxidation, TEM of the solution hardly give any features, suggesting that the nanofibers of **3** dissociate completely upon the oxidation. According to Figure 2B, the CD spectra also agree with the dissociation of the nanofibers of **3** caused by the oxidation. Particularly, the significant decrease of the CD signals of the far UV region (185–260nm), due to gel-sol transition, indicate that the secondary structures resulted from the peptide motif of **3** in the gel phase largely dissociate in the solution phase resulted from the oxidation of **3**. Little change of the CD signals originated from naphthalene at the near UV region (260–350nm) and the slightly increase of the CD signals originated from metal-to-ligand charge transfer (MLCT) (> 450 nm) imply that the chiral center on the peptides induce these CD signals (ICD),[25] which are less sensitive to the loss of the secondary structures. These results indicate that the redox change of the metal center of **3** induced transition of self-assembled structure of **3** in water.

HRTEM of the hydrogel of **3** (Fig. 3A) reveal an unexpected result that the diameters of the nanofibers of **3** (3.1±0.1 nm) are narrower than those (5.8±0.1 nm, Fig. S7) of the hydrogel of **1** despite that **1** has a much smaller molecular size (Fig. S12) than that of **3**. To understand the superstructure of the nanofibers formed by self-assembly of **3**, we evaluate the conformations and the molecular dimension of **3**. According to the minimized conformation calculated by molecular mechanics (MM), **3** has a dimension of 37.3 Å × 24.2 Å × 15.6 Å (Scheme 1), which suggests that the nanofibers in the hydrogel of **3** have the width of a single molecule of **3**. Figure 3B shows a plausible model of the nanofibers of **3**, in which the intermolecular aromatic-aromatic interactions from the overlaps of phenyl and/or naphthyl groups between **3** to result in the supramolecular chains (Fig. 3C). These 1D intermolecular interactions favor the formation of nanofibers at the exceptional low concentration of **3** (0.00625% (w/v), Fig. S3) before **3** reaches the minimum gelation concentration (0.1% (w/v)) at pH = 1 (Fig. S1). TEM images (Fig. S4) also indicate that **3** self-assembles to form nanofibers at the minimum concentrations of 0.1% (w/v) and pH of 7. There is little difference among the nanofibers formed by **3** in water even when they are formed under different conditions (Fig. S4). This observation agrees with the 1D model (Fig. 3B). Besides the octahedral geometry may disfavor the packing of the molecular nanofibers to form bundles, the charge repulsion between the ruthenium complexes also likely contributes to the separation of the molecular nanofibers. In addition, except two pairs of intramolecular hydrogen bonds formed by amide groups and hydroxyl groups of **3**, the remaining amide groups and hydroxyl groups would be available for forming hydrogen bonds with water molecules (Fig. 3C). These interactions allow the supramolecular chains, even at a relatively low molecule density, to hold considerable amount of water, which results in a hydrogel at a rather low minimal gelation concentration of **3**. Moreover, this kind of 1D intermolecular interaction resulted from motif **1** also contributes to a similar trend that slightly lower storage moduli of the hydrogel of **3** than that of the hydrogel of **1** at the same concentration and pH = 7 (Fig. S9).

In conclusion, this work, as the first example of ruthenium complex based supramolecular hydrogelators, illustrates a useful approach that incorporates functional metal complexes

into peptide-based hydrogelators for the development of multifunctional self-assembly system and materials. Although the molecular model of the nanofibers of **3** is tentative, the single molecular width of the nanofibers should be beneficial for studying the interaction of the supramolecular nanofibers with other molecules/targets. Interestingly, consisting of the tripeptide motifs, **3** exhibits little affinity to nucleic acids (Fig. S10), thus becoming cell compatible at relative high concentration (Fig. S11). This feature, which agrees well with the origin of the cytotoxicity of polypyridyl ruthenium complex,[21] may allow **3** to serve as a multipurpose hydrogelator to find applications in live cell imaging (Fig. 4). In fact, TEM reveals that the molecules of **3** are able to form nanofibers (Fig. S6) at 200 μM in cell culture medium, suggesting that the nanofibers of **3** also enter the cells. Moreover, we envision that, with the future advance of the fluorescent imaging techniques, the long fluorescence life-time of $[Ru(bipy)_3]^{2+}$ derivative[26] may allow the use of single-molecular width nanofibers of **3** to elucidate the interaction between these supramolecular nanofibers with proteins in live cells.

Supplementary Material

Refer to Web version on PubMed Central for supplementary material.

Acknowledgments

References

1. (a) Lehn JM. Angew Chem Intl Ed. 1990; 29:1304.(b) Whitesides GM, Mathias JP, Seto CT. Science. 1991; 254:1312. [PubMed: 1962191] (c) Hasenknopf B, Lehn JM, Boumediene N, DupontGervais A, VanDorsselaer A, Kneisel B, Fenske D. J Am Chem Soc. 1997; 119:10956.(d) Whitesides GM, Grzybowski B. Science. 2002; 295:2418. [PubMed: 11923529]

2. Estroff LA, Hamilton AD. Chem Rev. 2004; 104:1201. [PubMed: 15008620]

3. (a) Yang Z, Liang G, Xu B. Acc Chem Res. 2008; 41:315. [PubMed: 18205323] (b) Zhang Y, Gu HW, Yang ZM, Xu B. J Am Chem Soc. 2003; 125:13680. [PubMed: 14599204] (c) Toledano S, Williams RJ, Jayawarna V, Ulijn RV. J Am Chem Soc. 2006; 128:1070. [PubMed: 16433511] (d) Nagarkar RP, Hule RA, Pochan DJ, Schneider JP. J Am Chem Soc. 2008; 130:4466. [PubMed: 18335936] (e) Bowerman CJ, Nilsson BL. J Am Chem Soc. 2010; 132:9526. [PubMed: 20405940]

4. (a) Li XM, Kuang Y, Shi JF, Gao Y, Lin HC, Xu B. J Am Chem Soc. 2011; 133:17513. [PubMed: 21928792] (b) Mukhopadhyay S, Maitra U, Ira Krishnamoorthy G, Schmidt J, Talmon Y. J Am Chem Soc. 2004; 126:15905. [PubMed: 15571416] (c) Vemula PK, Li J, John G. J Am Chem Soc. 2006; 128:8932. [PubMed: 16819889] (d) Appel EA, Biedermann F, Rauwald U, Jones ST, Zayed JM, Scherman OA. J Am Chem Soc. 2010; 132:14251. [PubMed: 20845973] (e) Johnson EK, Adams DJ, Cameron PJ. J Am Chem Soc. 2010; 132:5130. [PubMed: 20307067] (f) Channon KJ, Devlin GL, Magennis SW, Finlayson CE, Tickler AK, Silva C, MacPhee CE. J Am Chem Soc. 2008; 130:5487. [PubMed: 18376824]

5. (a) Pouget E, Fay N, Dujardin E, Jamin N, Berthault P, Perrin L, Pandit A, Rose T, Valery C, Thomas D, Paternostre M, Artzner F. J Am Chem Soc. 2010; 132:4230. [PubMed: 20199027] (b) Boekhoven J, Koot M, Wezendonk TA, Eelkema R, van Esch JH. J Am Chem Soc. 2012; 134:12908. [PubMed: 22823592] (c) Cheetham AG, Zhang P, Lin Y-a, Lock LL, Cui H. J Am Chem Soc. 2013; 135:2907. [PubMed: 23379791] (d) Li JY, Kuang Y, Gao Y, Du XW, Shi JF, Xu B. J Am Chem Soc. 2013; 135:542. [PubMed: 23136972]

6. Gao Y, Kuang Y, Guo ZF, Guo ZH, Krauss IJ, Xu B. J Am Chem Soc. 2009; 131:13576. [PubMed: 19731909]

7. (a) Kisiday J, Jin M, Kurz B, Hung H, Semino C, Zhang S, Grodzinsky AJ. Proc Natl Acad Sci U S A. 2002; 99:9996. [PubMed: 12119393] (b) Silva GA, Czeisler C, Niece KL, Beniash E, Harrington

DA, Kessler JA, Stupp SI. Science. 2004; 303:1352. [PubMed: 14739465] (c) Li XM, Kuang Y, Lin HC, Gao Y, Shi JF, Xu B. Angew Chem Intl Ed. 2011; 50:9365.(d) Zhou M, Smith AM, Das AK, Hodson NW, Collins RF, Ulijn RV, Gough JE. Biomaterials. 2009; 30:2523. [PubMed: 19201459]

8. (a) Wada A, Tamaru S, Ikeda M, Hamachi I. J Am Chem Soc. 2009; 131:5321. [PubMed: 19351208] (b) Kiyonaka S, Sada K, Yoshimura I, Shinkai S, Kato N, Hamachi I. Nat Mater. 2004; 3:58. [PubMed: 14661016] (c) Chen J, McNeil AJ. J Am Chem Soc. 2008; 130:16496. [PubMed: 19049448] Gao Y, Shi JF, Yuan D, Xu B. 2012; 3:1033.Chen SJ, Chen LJ, Yang HB, Tian H, Zhu WH. J Am Chem Soc. 2012; 134:13596. [PubMed: 22881042]

9. Cui HG, Webber MJ, Stupp SI. Biopolymers. 2010; 94:1. [PubMed: 20091874]

10. (a) Terech P, Weiss RG. Chem Rev. 1997; 97:3133. [PubMed: 11851487] (b) van Esch JH, Feringa BL. Angew Chem Intl Ed. 2000; 39:2263.

11. (a) Lloyd GO, Steed JW. Nat Chem. 2009; 1:437. [PubMed: 21378911] (b) Piepenbrock MOM, Clarke N, Steed JW. Langmuir. 2009; 25:8451. [PubMed: 20050042]

12. (a) Tam AYY, Wong KMC, Yam VWW. J Am Chem Soc. 2009; 131:6253. [PubMed: 19354251] (b) Lu W, Law YC, Han J, Chui SSY, Ma DL, Zhu NY, Che CM. Chem Asian J. 2008; 3:59. [PubMed: 18058958]

13. Kishimura A, Yamashita T, Aida T. J Am Chem Soc. 2005; 127:179. [PubMed: 15631467]

14. Xing BG, Choi MF, Xu B. Chem Eur J. 2002; 8:5028. [PubMed: 12489537]

15. (a) Zhang SY, Yang SJ, Lan JB, Tang YR, Xue Y, You JS. J Am Chem Soc. 2009; 131:1689. [PubMed: 19159227] (b) Paulusse JMJ, van Beek DJM, Sijbesma RP. J Am Chem Soc. 2007; 129:2392. [PubMed: 17269773]

16. Gasnier A, Royal G, Terech P. Langmuir. 2009; 25:8751. [PubMed: 19374347]

17. Kuroiwa K, Shibata T, Takada A, Nemoto N, Kimizuka N. J Am Chem Soc. 2004; 126:2016. [PubMed: 14971934]

18. (a) Wang J, Chen Y, Law YC, Li MY, Zhu MX, Lu W. (b) Chui SSY, Zhu NY, Che CM. Chem-Asian J. 2011; 6:3011. [PubMed: 21898838] (c) Pan Y, Gao Y, Shi JF, Wang L, Xu B. J Mater Chem. 2011; 21:6804.(d) Joshi SA, Kulkarni ND. Chem Commun. 2009:2341.

19. (a) Zhu SS, Swager TM. Adv Mater. 1996; 8:497.(b) Kaes C, Katz A, Hosseini MW. Chem Rev. 2000; 100:3553. [PubMed: 11749322]

20. Suzuki M, Waraksa CC, Mallouk TE, Nakayama H, Hanabusa K. J Phys Chem B. 2002; 106:4227.

21. (a) Novakova O, Kasparkova J, Vrana O, Vanvliet PM, Reedijk J, Brabec V. Biochemistry. 1995; 34:12369. [PubMed: 7547981] (b) Pierroz V, Joshi T, Leonidova A, Mari C, Schur J, Ott I, Spiccia L, Ferrari S, Gasser G. J Am Chem Soc. 2012; 134:20376. [PubMed: 23181418]

22. (a) Gao WZ, Xing BG, Tsien RY, Rao JH. J Am Chem Soc. 2003; 125:11146. [PubMed: 16220906] (b) So MK, Xu CJ, Loening AM, Gambhir SS, Rao JH. Nat Biotechnol. 2006; 24:339. [PubMed: 16501578]

23. Maerker G, Case FH. 1958; 80:2745.

24. (a) Anderson S, Constable EC, Seddon KR, Turp JE, Baggott JE, Pilling MJ. J Chem Soc Dalton. 1985:2247.(b) Schwalbe M, Schafer B, Gorls H, Rau S, Tschierlei S, Schmitt M, Popp J, Vaughan G, Henry W, Vos JG. Eur J Inorg Chem. 2008:3310.(c) Sun YL, Machala ML, Castellano FN. Inorg Chim Acta. 2010; 363:283.

25. Shiraki T, Dawn A, Tsuchiya Y, Shinkai S. J Am Chem Soc. 2010; 132:13928. [PubMed: 20836560]
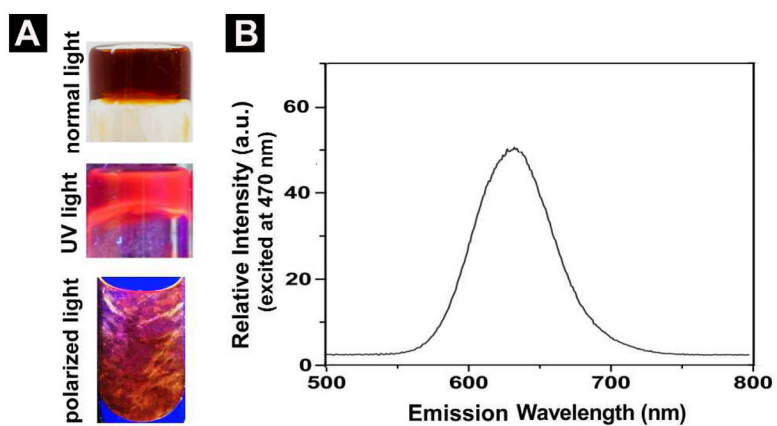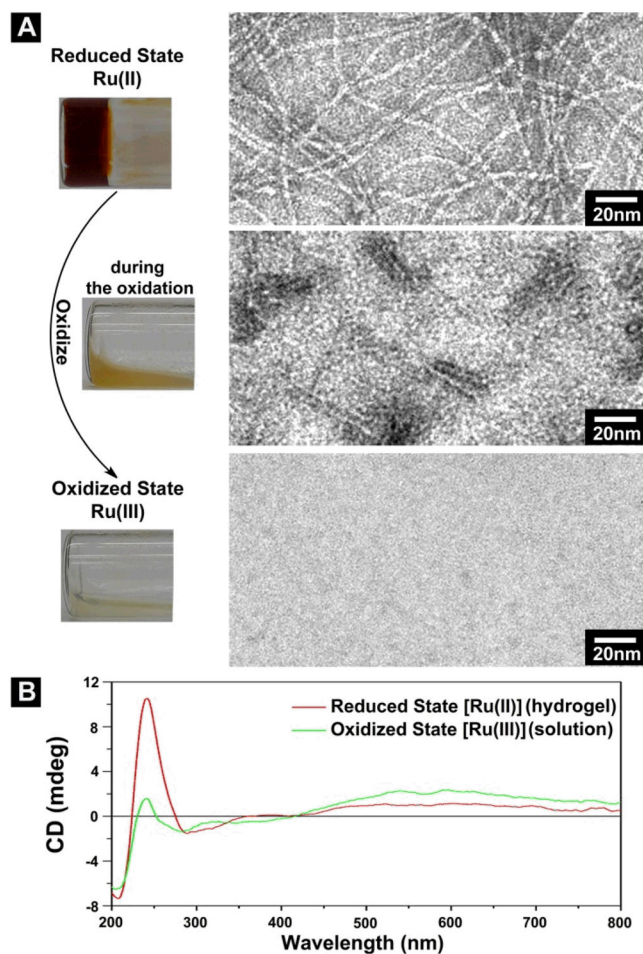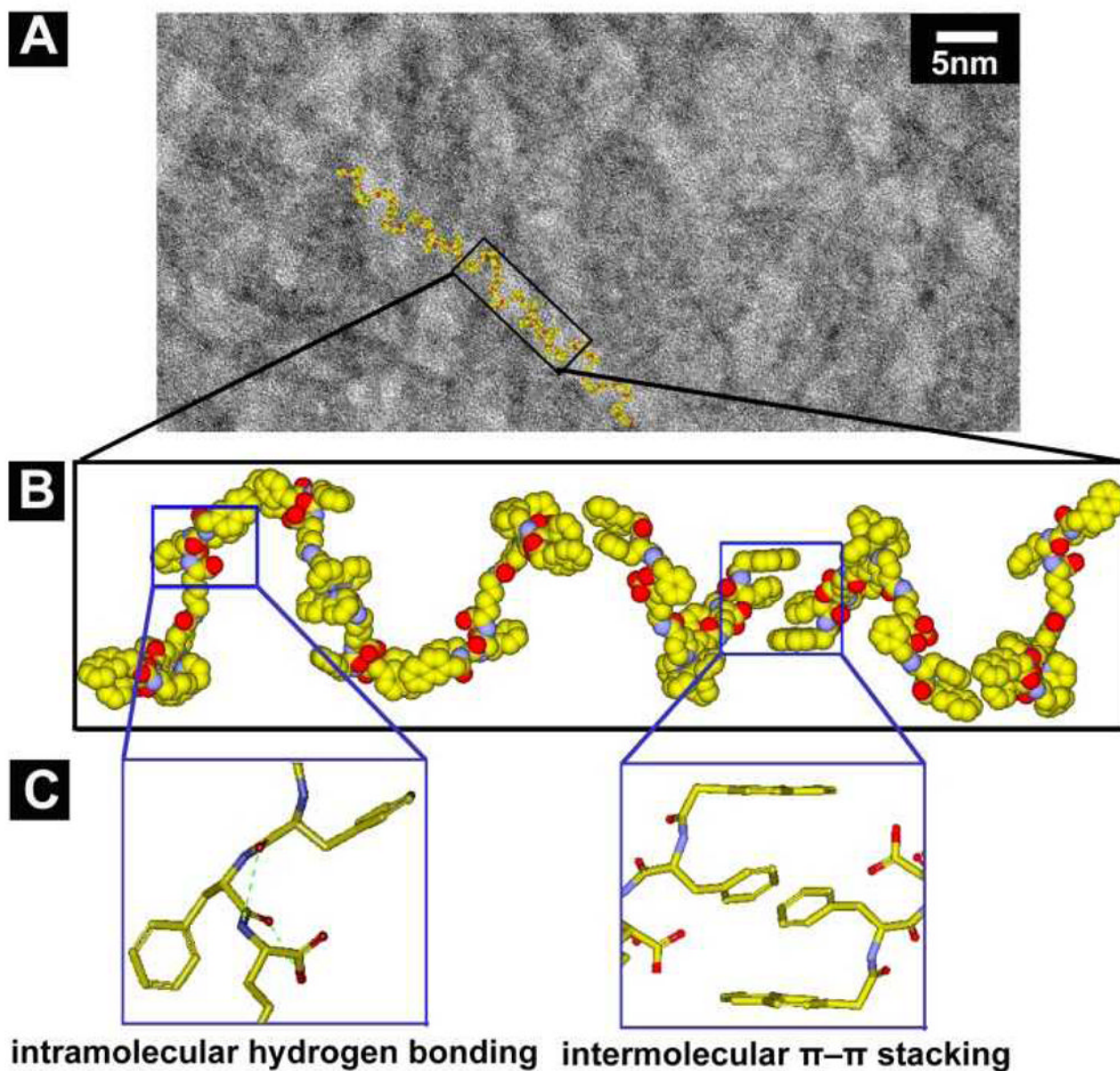
26. Yoshimizu H, Asakura T, Kaneko M. 1991; 192:1649.

FIGURE 1.
(A) Optical images of hydrogel formed by **3** (0.8% w/v) in water at pH = 7 under normal light, UV (long wavelength) light, and polarized light. (B) Emission (excited at 470 nm) spectrum of the hydrogel in (A).

FIGURE 2.
(A) Optical images of oxidation induced gel-sol transition and the TEM images corresponding to the samples at different states of transition. The hydrogel (reduced state) is formed by 0.8% (w/v) **3** in water at pH =1. Scale bar is 10 nm. (B) CD spectrum of the hydrogel (reduced state) and the solution (oxidized state).

Zhang et al. Page 8

NIH-PA Author Manuscript

NIH-PA Author Manuscript

NIH-PA Author Manuscript

FIGURE 3.
(A) High resolution TEM (HRTEM) image (scale bar is 5 nm) of the nanofibers in hydrogel of **3** (0.4% (w/v), pH = 1). (B) According to the TEM, a tentative molecular arrangement in the nanofibers of **3** (C) The illustrations of plausible intramolecular hydrogen bonds (green dash line) and intermolecular π–π stacking.

J Am Chem Soc. Author manuscript; available in PMC 2014 April 03.
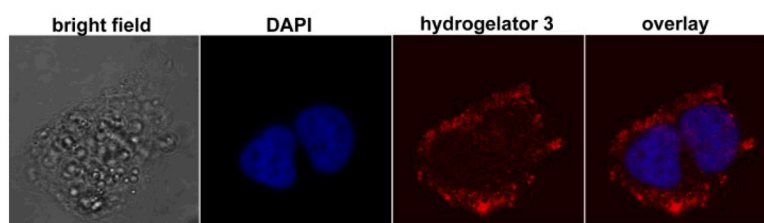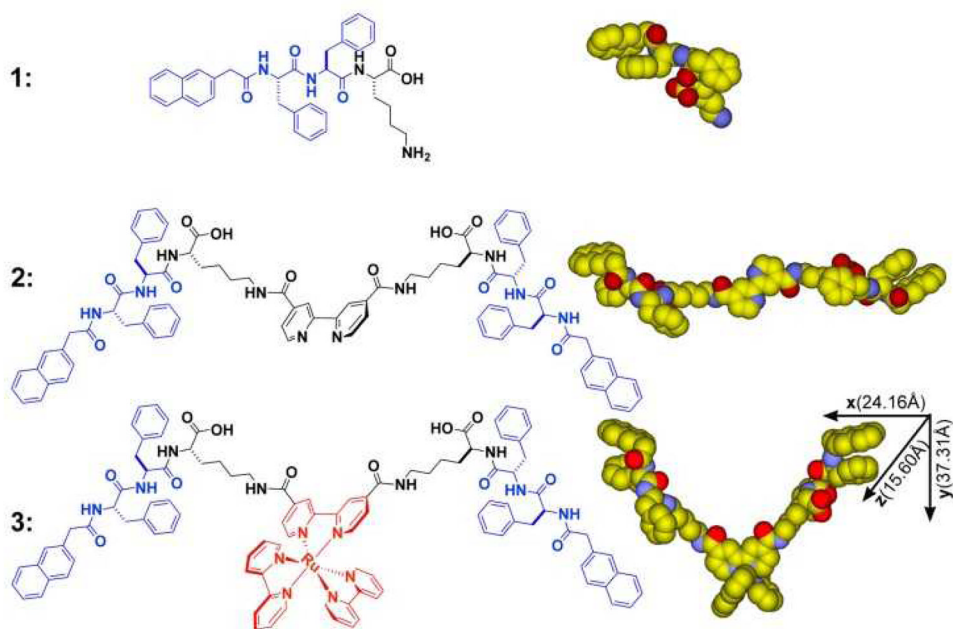
FIGURE 4.
The fluorescent image of a HeLa cell incubated with **3** (200 μM, 24h). From left to right: phase-contrast image, live cell stain DAPI (blue), luminescence emission of **3** (red) and overlay image.

SCHEME 1.
Molecular structures and CPK models of the self-assembly motif, the ligand, and the metallo-hydrogelator.